Steel and Composite Structures, Vol. 11, No. 6 (2011) 455-468
DOI: http://dx.doi.org/10.12989/scs.2011.11.6.455

Reinforced high-strength concrete square columns confined by aramid FRP jackets. part I: experimental study

Yuan-feng Wang[1]*, Yi-Shuo Ma[1], and Han-liang Wu[2]

[1)]*School of Civil Engineering, Beijing Jiaotong University, Beijing, 100044, PR China.*
[2)]*Bridge Technology Research Center, Research Institute of Highway, Ministry of Transportation, Beijing, 100088, PR China*

(Received May 27, 2010, Revised April 26, 2011, Accepted July 19, 2011)

Abstract. Although retrofitting and strengthening reinforced concrete (RC) columns by wrapping fiber reinforced polymer (FRP) composites have become a popular technique in civil engineering, the study on reinforced high-strength concrete (HSC) columns is still not sufficient. The objective of these companion papers is to investigate the mechanical properties of reinforced HSC square columns confined by aramid FRP (AFRP) jackets under concentric compressive loading. In the part I of these companion papers, an experiment was conducted on 54 confined RC specimens and nine unconfined plain specimens, the considered parameters were the concrete strength, the thickness of AFRP jackets, and the form of AFRP wrapping. The experimental process and results are presented in detail. Subsequently, some discussions on the confinement effect, failure modes, strength, and ductility of the columns are carried out.

Keywords: reinforcement; high-strength concrete (HSC); confined columns; fiber reinforced polymers (FRP); experimentation.

1. Introduction

Since the last quarter of the twentieth century, fiber reinforced polymer (FRP) composites have become popular materials for retrofitting and strengthening civil engineering structures (including buildings, bridges, and tunnels), due to their advantages such as high strength, good corrosion resistance, lightweight, ease of application, and so on.

One of the most efficient applications of FRP composites in civil engineering is the strengthening of concrete columns with externally wrapping FRP jackets. For FRP-confined concrete columns with square (or rectangular, wall-like) sections, some general conclusions have been drawn (Cheng *et al*. 2002, Teng and Lam 2004, Hassan and Chaallal 2007, Wu *et al*. 2007): (1) the confinement effect on the columns is directly related to the shape of columns' cross-section, the columns with square cross-section exhibit lower confinement effect than those with circular cross-section, when confined by a same amount of FRP jackets; (2) the confinement effect is more concentrated in regions close to the corners of columns, which is named as the arching action; (3) the corner radius directly influences the strength and ductility of columns; (4) the enhancements in the strength and ductility of columns increase as the strength and stiffness of FRP jackets increase.

* Corresponding author, Professor, E-mail: cyfwang@bjtu.edu.cn

Although FRP-confined concrete columns with square cross-section have been studied for about twenty years, there still exist several deficiencies, as explained in the following:

(1) Most of the studies concentrated on normal-strength concrete (NSC), while very few on high-strength concrete (HSC). HSC has been widely used in civil engineering predominantly for its high strength performance, but its application is limited by a concern regarding more serious brittleness when compared with NSC. It has been demonstrated that the ductility of HSC columns can be increased by the confinement attributed to FRP jackets (Li 2006, Almusallam 2007, Hadi 2007, Campione 2008).

(2) Most of the literatures were concerned with FRP-confined plain concrete columns, while only a few studies have investigated FRP-confined reinforced concrete (RC) columns. In practice, typical concrete columns usually incorporate longitudinal and lateral steel reinforcements. For FRP-confined RC columns, internal lateral steel stirrups and external FRP jackets offer confinements on concrete cores by different manners. The internal steel stirrups provide constant confinement after they yield because of the elastic-plastic property of steel, while the external FRP jackets provide increasing confinement until they break because of the linear elastic property of FRP. Compared with the steel stirrups, the FRP jackets are more effective on supporting the longitudinal steel reinforcements in the columns against buckling (Tastani *et al*. 2006). Consequently, RC columns confined by FRP jackets behave differently from concrete columns confined by steel stirrups or FRP jackets alone. In recent years, although some experimental studies on FRP-confined reinforced NSC columns with square sections have been carried out, there are few on FRP-confined reinforced HSC square columns.

(3) The general categories of FRP used in the previous studies were carbon FRP (CFRP) and glass FRP (GFRP), while aramid FRP (AFRP) was rarely taken into account. Actually, the tensile strength of AFRP is 20% lower than that of CFRP, but the elongation-to-break ratio of AFRP is 60% higher than that of CFRP (Yu 2004). In addition, compared with GFRP, AFRP has slightly higher elongation-to-break ratio, but much higher strength (Burgoyne and Balafas 2007). Thus, AFRP is more appropriate for the applications that require both higher strength and larger deformation, even though AFRP's cost is slightly higher than that of CFRP and GFRP. In recent years, some researchers had reported their works on AFRP confined concrete columns. Wu *et al*. (2009), Wang and Wu (2010) studied AFRP confined plain concrete columns with circular and square cross-section, and found the AFRP sheets can provided significant strengthening in strength of HSC columns under uniaxial compression. Wu and Wang (2010) tested 45 specimens and proposed a modified prediction model for AFRP confined RC columns with circular cross-section.

The objective of these companion papers is to investigate the mechanical properties of reinforced HSC square columns confined by AFRP jackets. The part I of these companion papers is an experimental study. 54 RC columns confined by AFRP jackets and nine additional unconfined plain concrete columns, as the reference specimens, were tested to failure under concentric compressive loading. The following parameters were considered: concrete strength, thickness of AFRP jackets, and form of AFRP wrapping. Subsequently, the confinement effects, failure modes, strength, and ductility of the tested columns are discussed.

2. Experimental program

2.1. Geometric characteristics of specimens

All the specimens, including 54 AFRP-confined specimens and nine plain specimens, had a same

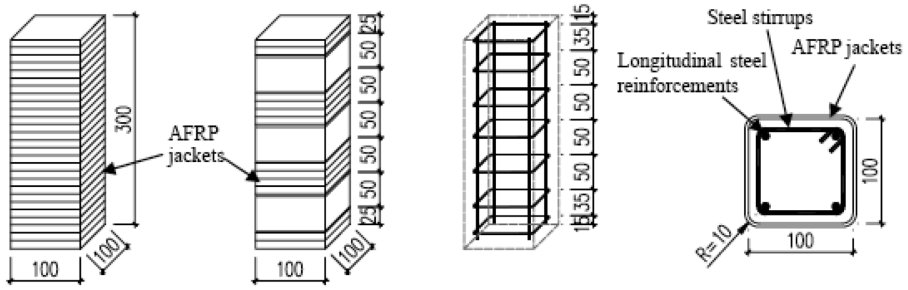

(a) Specimen dimensions and forms of AFRP wrapping (b) Reinforcement cage

Fig. 1. Specimen dimensions and form of AFRP wrapping, and Reinforcement cage (mm)

square cross-section with 100 mm in width and 300 mm in height [as shown in Fig. 1(a)]. To prevent stress concentrations in the external AFRP jackets, the corners of specimens were rounded to a 10 mm radius. The reinforcement cage in are RC specimen consisted of four longitudinal steel reinforcements and seven lateral steel stirrups [as shown in Fig. 1(b)]. The longitudinal steel reinforcements were 8 mm in diameter and placed at the corners of steel stirrups. The lateral steel stirrups were 4 mm in diameter and placed with a spacing of 35 or 50 mm. The clear thickness of cover concrete was 13 mm. The external AFRP jackets were wrapped around the specimens in either a continuous or discontinuous form, and the principal direction of AFRP's fibers was normal to the longitudinal axes of specimens [as shown in Fig. 1(a)]. Before installing the AFRP sheets, all resin components provided by the AFRP system manufacturer were mixed until the color streaks of different components were eliminated. The trimmed AFRP sheets were bonded to the concrete surface, after the sheets were impregnated with the prepared resin. An additional overlapping length of 100 mm was required to provide a sufficient anchorage, and special attention was paid to ensuring no voids between the AFRP system and the concrete. Before tested, all the AFRP-confined specimens were cured for at least seven days in a controlled temperature (20 ± 3^{o}C).

2.2. Properties of materials

The concrete used was prepared in the laboratory. There were three different grades of concrete strength, the 28-day average compressive strengths of unconfined plain specimens (f_{c0}) were 46.43, 78.50, and 101.18 MPa, respectively. The yield strengths were 260 MPa for the longitudinal steel reinforcements (f_{yl}) and 265 MPa for the lateral steel stirrups (f_{yh}). The elastic moduli of longitudinal steel reinforcements (E_{sl}) and lateral steel stirrups (E_{sh}) were both 2×10^5 MPa. The AFRP material used was of the ASF-60 series produced by Dupont Co., with the properties provided by the manufacturer as shown in Table 1, where f_f = tensile strength of AFRP (MPa); E_f = elastic modulus of AFRP (MPa); and ε_{fu} = ultimate rupture strain of AFRP. The available thicknesses of AFRP jackets were 0.286, 0.572, and 0.858 mm for selection. Presented in Table 2 are the properties of the specimens, where ε_{c0} = compressive strain of unconfined specimens corresponding to f_{c0}; and t_f = thickness of AFRP jackets (mm).

2.3. Instruments of loading and measuring

All the specimens were loaded to failure under monotonic axial compressive loading in a testing machine with a limit compressive load capacity of 3000 kN. A spherical support was used in order to

Table 1 Mechanical properties of AFRP provide by the manufacturer

Type of AFRP	f_f (MPa)	E_f (MPa)	ε_{fu}
AFS-60	2,060	118×10^3	1.77%

Table 2 Properties of the specimens

Specimen designation	f_{co} (MPa)	ε_{c0} (10^{-3})	Form of wrapping	t_{co} (mm)	Number. of specimens
L-Pain Concrete			-	0.000	3
L-C-1			Continuous	0.286	3
L-C-2			Continuous	0.572	3
L-C-3	46.43	2.55	Continuous	0.858	3
L-D-1			Discontinuous	0.286	3
L-D-2			Discontinuous	0.572	3
L-D-3			Discontinuous	0.858	3
M-Pain Concrete			-	0.000	3
M-C-1			Continuous	0.286	3
M-C-2			Continuous	0.572	3
M-C-3	78.50	4.51	Continuous	0.858	3
M-D-1			Discontinuous	0.286	3
M-D-2			Discontinuous	0.572	3
M-D-3			Discontinuous	0.858	3
H-Pain Concrete			-	0.000	3
H-C-1			Continuous	0.286	3
H-C-2			Continuous	0.572	3
H-C-3	101.18	4.56	Continuous	0.858	3
H-D-1			Discontinuous	0.286	3
H-D-2			Discontinuous	0.572	3
H-D-3			Discontinuous	0.858	3

acquire a concentric load. The load was applied at a mode of 0.15 MPa/s in stress, then changed to 0.001 ε/s in strain after exceeding 80% of compressive strength of the unconfined specimens.

The axial compressive load was measured by a pressure transducer system installed into the testing machine with 0.001 kN accuracy, and the nominal axial stress (σ, MPa) is obtained through dividing the measured load by the cross-section area of specimens. The axial compressive displacement was measured by an electronic extensometer with 100 mm gauge length and 0.01 mm accuracy, which was mounted at the mid-height of specimens (as shown in Fig. 2), and the nominal axial strain (ε, m/m) is obtained

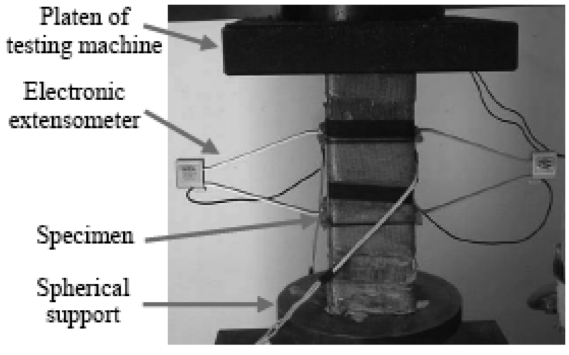

Fig. 2. Instruments of measuring

through dividing the measured displacement by 100 mm.

3. Experimental results

The measured nominal axial stress-strain curves of confined specimens are shown in Fig. 3 (note: only one measured curves is presented for the sake of clear illustrating), it is observed that the curves are bilinear except those of several groups (M-C-2, H-C-1, H-D-1, H-D-2 and H-D-3). As pointed out

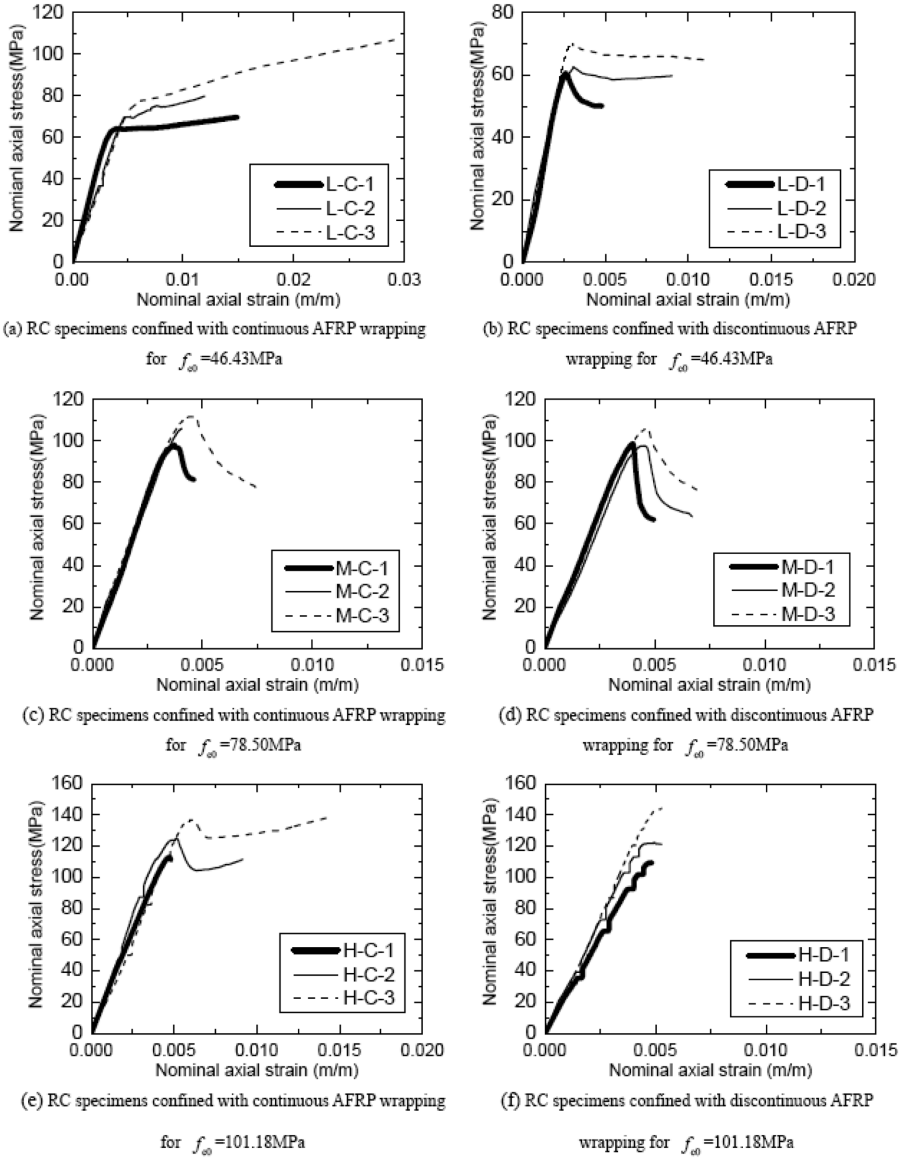

(a) RC specimens confined with continuous AFRP wrapping for f_{c0}=46.43MPa

(b) RC specimens confined with discontinuous AFRP wrapping for f_{c0}=46.43MPa

(c) RC specimens confined with continuous AFRP wrapping for f_{c0}=78.50MPa

(d) RC specimens confined with discontinuous AFRP wrapping for f_{c0}=78.50MPa

(e) RC specimens confined with continuous AFRP wrapping for f_{c0}=101.18MPa

(f) RC specimens confined with discontinuous AFRP wrapping for f_{c0}=101.18MPa

Fig. 3 Nominal axial stress-strain curves of the confined specimens

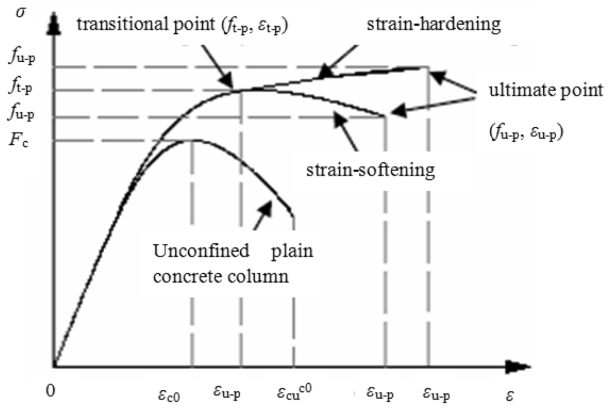

Fig. 4 Typical stress-strain curve of confined concrete columns

by some researchers, such as Tan (2002), Teng *et al*. (2003), Debaiky *et al*. (2007), a typical bilinear stress-strain curve for confined concrete columns can be determined with two key points, one is the transition-point (f_{t-p}, ε_{t-p}) and the other is the ultimate-point (f_{u-p}, ε_{u-p}), where f_{t-p}, ε_{t-p} = transitional strength (MPa) and transitional strain (m/m) for AFRP-confined reinforced HSC columns, respectively; and f_{u-p}, ε_{u-p} = ultimate strength (MPa) and ultimate strain (m/m), as shown in Fig. 4, respectively. It is also shown that the nominal axial stress-strain curves can be classified into two types: one is the strain-hardening curve which continues to increase with a reduced slope after reaching its transitional point, and the other is the strain-softening curve which decreases after reaching its transitional point. The experimental data are presented in Table 3.

Table 3 Experimental results of the specimens

Specimen designation	f_l(MPa)	f_{t-p}(MPa)	f_{t-p}/f_{c0}	$\varepsilon_{t-p}(10^{-3})$	$\varepsilon_{t-p}/\varepsilon_{c0}$	f_{u-p}(MPa)	f_{u-p}/f_{c0}	$\varepsilon_{u-p}(10^{-3})$	$\varepsilon_{u-p}/\varepsilon_{c0}$
L-Pain Concrete	0.00	46.27	1.00	2.21	1.00	32.39	0.70	3.71	1.68
		47.30	1.00	2.79	1.00	33.11	0.70	4.64	1.66
		45.72	1.00	2.65	1.00	32.00	0.70	4.48	1.69
L-C-1	6.83	62.67	1.35	3.59	1.41	-	-	-	-
		64.23	1.38	3.92	1.54	69.78	1.50	14.87	5.83
		66.02	1.42	3.56	1.40	71.85	1.55	13.11	5.14
L-C-2	13.48	62.85	1.35	3.75	1.47	-	-	-	-
		69.70	1.50	4.73	1.85	79.81	1.72	11.95	4.69
		70.78	1.52	6.24	2.45	-	-	-	-
L-C-3	20.13	77.80	1.68	6.28	2.46	106.84	2.30	29.04	12.79
		71.74	1.55	5.94	2.33	88.71	1.91	28.07	11.01
		70.82	1.53	6.98	2.74	91.41	1.97	25.61	10.04
L-D-1	2.80	60.63	1.31	2.62	1.03	50.01	1.08	4.81	1.89
		48.48	1.04	3.11	1.22	45.36	0.98	5.24	2.05
		63.34	1.36	2.51	0.98	47.53	1.02	4.60	1.80
L-D-2	5.42	60.97	1.31	3.33	1.31	57.29	1.23	8.42	3.30
		62.66	1.35	3.08	1.21	59.74	1.29	9.02	3.54
		61.14	1.32	3.95	1.55	60.59	1.30	10.90	4.27
L-D-3	8.04	65.29	1.41	3.16	1.24	63.84	1.37	8.69	3.41
		65.65	1.41	3.26	1.28	61.21	1.32	8.14	3.19
		70.11	1.51	2.99	1.17	64.93	1.40	10.96	4.30

Table 3 Continued

Specimen designation	f_l(MPa)	$f_{t\text{-}p}$(MPa)	$f_{t\text{-}p}/f_{c0}$	$\varepsilon_{t\text{-}p}(10^{-3})$	$\varepsilon_{t\text{-}p}/\varepsilon_{c0}$	$f_{u\text{-}p}$(MPa)	$f_{u\text{-}p}/f_{c0}$	$\varepsilon_{u\text{-}p}(10^{-3})$	$\varepsilon_{u\text{-}p}/\varepsilon_{c0}$
M-Pain Concrete	0.00	78.01	1.00	4.45	1.00	54.61	0.70	6.07	1.36
		80.27	1.00	4.71	1.00	56.19	0.70	6.37	1.35
		77.22	1.00	4.37	1.00	54.05	0.70	5.98	1.37
M-C-1	6.83	93.39	1.19	4.15	0.92	72.65	0.93	5.00	1.11
		98.63	1.26	4.21	0.93	61.09	0.78	8.27	1.83
		98.12	1.25	4.02	0.89	81.34	1.04	4.62	1.02
M-C-2	13.48	102.84	1.31	4.29	0.95	-	-	-	-
		106.10	1.35	4.05	0.90	-	-	-	-
		101.11	1.29	4.12	0.91	-	-	-	-
M-C-3	20.13	111.76	1.42	4.39	0.97	78.41	1.00	7.51	1.67
		103.28	1.32	4.13	0.92	87.34	1.11	6.15	1.36
		103.62	1.32	4.44	0.98	80.30	1.02	9.11	2.02
M-D-1	2.80	99.13	1.26	4.24	0.93	63.33	0.81	5.70	1.26
		98.70	1.26	4.29	0.95	62.02	0.79	4.65	1.03
		91.31	1.16	4.43	0.98	58.19	0.74	5.44	1.21
M-D-2	5.42	97.70	1.25	4.53	1.00	63.53	0.81	6.69	1.48
		95.55	1.22	4.32	0.96	60.84	0.77	6.58	1.46
		101.11	1.29	4.21	0.93	67.06	0.85	6.16	1.37
M-D-3	8.04	106.17	1.35	4.67	1.04	76.02	0.97	7.02	1.56
		98.63	1.26	3.97	0.88	61.21	0.78	8.49	1.88
		103.62	1.32	4.72	1.05	80.30	1.02	9.41	2.09
H-Pain Concrete	0.00	98.48	1.00	4.31	1.00	68.94	0.70	5.51	1.28
		104.56	1.00	4.86	1.00	73.19	0.70	6.13	1.26
		100.50	1.00	4.51	1.00	70.35	0.70	5.74	1.27
H-C-1	6.83	120.22	1.19	3.76	0.82	-	-	-	-
		106.65	1.05	3.62	0.79	-	-	-	-
		113.01	1.12	4.73	1.04	-	-	-	-
H-C-2	13.48	128.55	1.27	5.15	1.13	139.40	1.38	16.82	3.69
		128.76	1.27	5.23	1.15	105.47	1.04	8.28	1.82
		125.00	1.24	5.14	1.13	111.52	1.10	9.15	2.01
H-C-3	20.13	136.91	1.35	6.01	1.32	138.29	1.37	14.35	3.15
		136.15	1.35	5.18	1.14	124.46	1.23	9.22	2.02
		138.36	1.37	4.63	1.02	152.12	1.50	10.39	2.28
H-D-1	2.80	112.17	1.11	4.29	0.94	-	-	-	-
		109.50	1.08	4.83	1.06	-	-	-	-
		100.86	1.00	4.17	0.91	-	-	-	-
H-D-2	5.42	124.99	1.24	5.30	1.16	-	-	-	-
		122.34	1.21	4.97	1.09	-	-	-	-
		132.44	1.31	4.21	0.92	-	-	-	-
H-D-3	8.04	128.80	1.27	4.77	1.05	-	-	-	-
		144.41	1.43	5.27	1.16	-	-	-	-
		129.03	1.28	5.55	1.22	-	-	-	-

Note : "-" represents the test value is not available.

4. Discussions

4.1. Confinement effects

Under axial compressive loading, the concrete cores of reinforced HSC square columns confined by AFRP jackets dilate transversely, however the dilation is restrained because of the confinement effects

attributed to steel stirrups and AFRP jackets. The distributions of confining stress on the concrete core, due to the internal steel stirrups and the external AFRP jackets, is assumed as the principle of arching action both in the cross-section and in the vertical-section of columns (Mander *et al.* 1988, Restrepo and De Vino 1995). As a result, the concrete core a of specimen can be divided into an effectively confined area and several ineffectively confined areas, are shown in Fig. 5. For the configuration of steel stirrups in this experiment, an equivalent confining stress representing the confinement effect due to the internal steel stirrups is given by (Mander *et al*. 1988)

$$f_{ls} = \frac{f_{yh}A_{sh}}{B_c S_h} \cdot \frac{\left[1-\frac{2}{3}\frac{(B_s)^2}{(B_c)^2}\right]\left[1-\frac{S_h^*}{2B_c}\right]^2}{1-\rho_{cc}} \tag{1}$$

where B_s = clear spacing between adjacent longitudinal steel reinforcements (mm); B_c = core dimension to centerlines of steel stirrups (mm); S_h^* = clear vertical spacing between adjacent steel stirrups (mm); S_h= center to center spacing between adjacent steel stirrups (mm); ρ_{cc} = ratio of area of longitudinal steel reinforcements to area of core of section, $\rho_{cc} = A_{sl} / (B_c)^2$; A_{sl} = cross-section area of longitudinal steel reinforcements (mm^2); and A_{sh} = cross-section area of steel stirrups (mm^2).

An equivalent confining stress representing the confinement effect due to external FRP jackets is given by

$$f_{lf} = k_e \frac{\left[S_f + \left(1-\frac{S_f^*}{2B}\right)^2 S_f^*\right]}{S_f + S_f^*} \times \frac{S_f}{S_f + S_f^*} \times \frac{2f_f t_f}{B} \tag{2}$$

$$k_e = \frac{[B^2 - (4R^2 - \pi R^2)] - A_{sl} - \frac{2}{3}(B-2R)^2}{B^2 - (4R^2 - \pi R^2) - A_{sl}} \tag{3}$$

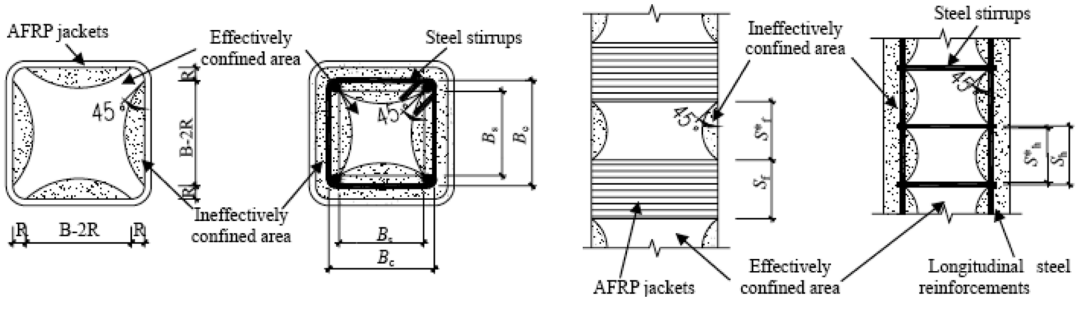

(a) Distributions of confining stress in cross section attributed to AFRP jackets and steel stirrups respectively

(b) Distributions of confining stress in vertical section attributed to AFRP jackets and steel stirrups respectively

Fig. 5 Effectively and ineffectively confined areas in cross section and vertical section

where k_e = effectiveness coefficient for FRP confinement; B = width of cross section (mm); R = corner radius of cross section (mm); S_f^* = clear vertical spacing between adjacent AFRP jackets (mm, which is equal to zero for the specimens confined with continuous AFRP wrapping); and S_f = width of AFRP

(a) Rupture of AFRP jackets for RC specimens confined with discontinuous AFRP wrapping (L-D-1)

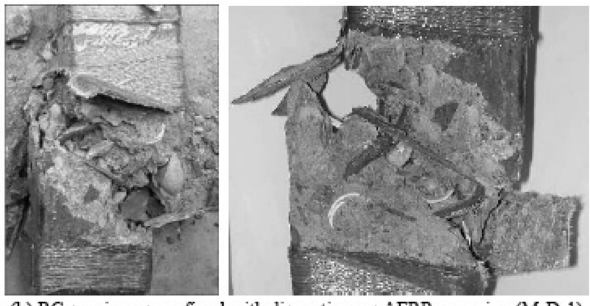

(b) RC specimens confined with discontinuous AFRP wrapping (M-D-1)

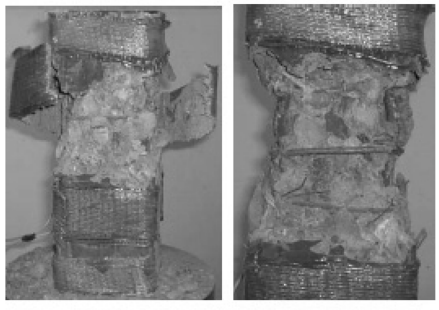

(c) RC specimens confined with discontinuous AFRP wrapping (M-D-3)

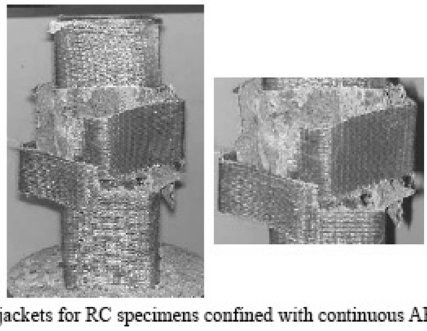

(d) Rupture of AFRP jackets for RC specimens confined with continuous AFRP wrapping (L-C-1)

Fig. 6 Failure modes

jackets (mm).

Considering the different areas confined by steel stirrups and AFRP jackets, as shown in Fig. 6, a total equivalent confining stress is defined as

$$f_l = \frac{(f_{ls}A_{cs} + f_{lf}A_{cf})}{A_{cf}} \tag{4}$$

where A_{cf} = ross-section area of concrete confined by the AFRP jackets (mm^2), $A_{cf} = B^2 - (4R^2 - \pi R^2)$; and A_{cs} = cross-section area of concrete confined by the steel stirrups (mm^2), $A_{cs} = B_s^2$.

4.2. Failure modes

For the specimens confined with discontinuous AFRP wrapping, during the early stage of loading process, there was no obvious change on the surfaces of specimens. From the middle stage of loading process, the specimens generated some noise, which was probably caused by micro-cracking of concrete by shifting of aggregates and by splitting of resins. Near the end of loading process, a complete failure occurred accompanied by an explosive sound. The AFRP jackets ruptured at (or near) one or more corners of specimens, which was mainly caused by stress concentrations [as shown in Fig. 6 (a)]. When the thickness of AFRP jackets was small, there was lots of crushed concrete and the longitudinal steel reinforcements buckled at the location of the AFRP jackets rupturing [as shown in Fig. 6 (b)]. However, when the thickness of AFRP jackets was large, there was little of crushed concrete and the longitudinal steel reinforcements curved without buckling [as shown in Fig. 6 (c)]. For the specimens confined with continuous AFRP wrapping [as shown in Fig. 6 (d)], the experimental phenomena were similar to those of the specimens confined with discontinuous AFRP wrapping except for the buckling of longitudinal steel reinforcements, because the FRP jackets were remarkably effective in precluding premature buckling of longitudinal steel reinforcements in FRP-confined RC columns (Wang and Hsu 2008). Additionally, the experimental results show that the AFRP-confined RC columns exhibit similar failure modes as FRP-confined plain concrete columns, as mentioned by Almusallam (2007).

4.3. Ductility

For the specimens confined with continuous AFRP wrapping, it can be observed (as shown in Table. 3) that the ultimate strain ($\varepsilon_{u\text{-}p}$) increases when the confining stress increases, and the increment is more notable when the concrete strength of specimens is lower. That is, the value of $\varepsilon_{u\text{-}p} / \varepsilon_{c0}$ is 4.69~12.79 for concrete strength of f_{c0} = 46.43 MPa, 1.02~2.02 for f_{c0} = 78.50 MPa, and 2.02~3.69 for f_{c0} = 101.18 MPa. Meanwhile, when the confining stress increases, the transitional strain ($\varepsilon_{t\text{-}p}$) increases slightly only for the specimens with the concrete strength of 46.43 MPa, the value of $\varepsilon_{t\text{-}p} / \varepsilon_{c0}$ is 1.40~2.74; and for the specimens with concrete strengths of 78.50 and 101.18 MPa, $\varepsilon_{t\text{-}p} / \varepsilon_{c0}$ is 0.89~1.32. For the specimens confined with discontinuous AFRP wrapping, $\varepsilon_{u\text{-}p}$ increases slightly when the confining stress increases. Whereas, $\varepsilon_{t\text{-}p}$ is always almost equal to ε_{c0}.

4.4. Strength

For the specimens confined with continuous AFRP wrapping, the transitional strength ($f_{t\text{-}p}$) and the ultimate strength ($f_{u\text{-}p}$) increase when the confining stress increases, and the increments are more

notable when the concrete strength is lower. That is, the value of $f_{t\text{-}p}$ / f_{c0} is 1.35~1.68 for concrete strength of f_{c0} = 46.43 MPa, 1.19~1.42 for f_{c0} = 78.50 MPa, and 1.05~1.37 for f_{c0} = 101.18 MPa; the value of $f_{u\text{-}p}$ / f_{c0} is 1.40~2.74 for concrete strength of f_{c0} = 46.43 MPa, 0.89~0.98 for f_{c0} = 78.50 MPa, and 0.82~1.15 for f_{c0}=101.18 MPa. For the specimens confined with discontinuous AFRP wrapping, the increments of $f_{t\text{-}p}$ and $f_{u\text{-}p}$ are slight when the confining stress increases.

5. Conclusions

1. The strength and ductility of reinforced HSC square columns can be enhanced by the confinement of external AFRP jackets, though the enhancements are slight for the columns confined with discontinuous AFRP wrapping.
2. The improvements in strength and ductility attributed to external AFRP jackets are greater when the concrete strength is lower.
3. For the columns confined with discontinuous AFRP wrapping, buckling of longitudinal steel reinforcements can be precluded effectively when the thickness of AFRP jackets is large. For the columns confined with continuous AFRP wrapping, no buckling does occur.

Acknowledgments

The writers would like to acknowledge the financial support provided by the National Natural Science Foundation (NSF) of China under Grant No. 50378002 and Science and Technology Program for West Part Transportation Construction of the Ministry of Transportation of China under Grant No. 200431800058. The supports provided by Beijing Jiaotong University and China Railway Co. Laboratory for the experiment, and the contribution of AFRP materials from Shenzhen Ocean Power Engineering Technology Co., Ltd. are also gratefully acknowledged.

References

Almusallam, T. H. (2007). "Behavior of normal and high-strength concrete cylinders confined with E-glass/epoxy composite laminates." *Compos. Part B: Eng.*, **38**(5), 629-639.

Burgoyne C. and Balafas L. (2007). "Why is FRP not a financial success?" *Proceeding of the FRPRCS-8 symposium*, Patras.

Campione, G. (2008). "Analytical model for high-strength concrete columns with square cross-section." *Struct. Eng. Mech.*, **28**(3), 295-316.

Cheng, H. L., Sotelino, E. D. and Chen, W. F. (2002). "Strength estimation for FRP wrapped reinforced concrete columns.". *Steel & Compos. Struct.*, **2**(1), 1-20.

Debaiky, A. S., Green, M. F. and Hope, B. B. (2007). "Modeling of corroded FRP-wrapped reinforced concrete columns in axial compression." *J. Compos. Constr.*, **11**(6), 556-564.

Hadi, M. N. S. (2007). "The behavior of FRP wrapped HSC columns under different eccentric loads." *Compos. Struct.*, **78**(4), 560-566.

Hassan, M. and Chaalal, O. (2007). "Fiber-reinforced polymer confined rectangular columns: assessment of models and design guidelines." *ACI Struct. J.*, **104**(6), 693-702.

Li, G. Q. (2006). "Experimental study of FRP confined concrete cylinder." *Eng. Struct.*, **28**(7), 1001-1008.

Mander, J. B., Priestley, J. N. and Park, R. (1988). "Theoretical stress-strain model for confined concrete." *J.*

Struct. Eng., **114**(8), 1804-1826.
Restrepo, J. I. and De Vino, B. (1995). "Enhancement of the axial load carrying capacity of reinforced concrete columns by means of fiberglass-epoxy jackets." *Proceedings of Advanced Composite Materials in Bridges and Structures II*, Montreal.
Tan, K. H. (2002). "Strength enhancement of rectangular reinforced concrete columns using fiber-reinforced polymer." *J. Compos. Constr.*, **6**(3), 175-183.
Tastani. S. P., Pantazopoulou, S. J., Zdoumba, D., Plakantaras, V. and Akritidis, E. (2006). "Limitations of FRP jacketing in confining old-type reinforced concrete members in axial compression." *J. Compos. Constr.*, **10** (1), 13-25.
Teng, J.G. and Lam, L. (2004). "Behaviour and modeling of FRP-confined concrete: a state-of-the-art review". *Proceeding of international symposium of confined concrete (ISCC-2004)*, Changsha.
Teng, M. H., Sotelino, E. D. and Chen, W. F.(2003). "Performance evaluation of reinforced concrete bridge columns wrapped with fiber reinforced polymer." *J. Compos. Constr.*, **7**(2), 83-92.
Wang, Y. C. and Hsu, K. (2008). "Design of FRP-wrapped reinforced concrete columns for enhancing axial load carrying capacity." *Compos. Struct.*, **82**(1), 132-139.
Wang, Y. F. and Wu, H. L. (2010). "Experimental investigation on square high-strength concrete short columns confined with AFRP sheets." *J. Compos. Constr.*, **14**(3), 346-351.
Wu, G., Wu, Z. S. and Lu, Z. T. (2007). "Design-oriented stress-strain model for concrete prisms confined with FRP composites." *Constr. Build. Mater.*, **21**(5), 1107-1121.
Wu, H. L. and Wang, Y. F.,(2010). "Experimental study on reinforced high-strength concrete short columns confined with AFRP sheets." *Steel. Compos. Struct.*, **10**(6), 501-516.
Wu, H. L., Wang, Y. F., Yu, L. and Li, X. R. (2009). "Experimental and computational studies on high-strength concrete circular columns confined by aramid fiber-reinforced polymer sheets." *J. Compos. Constr.*, **13**(2), 125-134.
Yu, G. (2004). "Study on the performance of AFRP-confined circular concrete column". Ms thesis, Harbin, Harbin Institute of Technology (in Chinese).

CC

Notation

The following symbols are used in this paper:

A_{cf} cross-section area of concrete confined by the AFRP jackets (mm^2);
A_{cs} cross-section area of concrete confined by the steel stirrups (mm^2);
A_{sl} cross-section area of longitudinal steel reinforcements (mm^2);
A_{sh} cross-section area of steel stirrups (mm^2);
B width of cross section (mm);
B_c concrete core dimension to center lines of perimeter steel stirrups (mm);
B_s clear spacing between adjacent longitudinal steel reinforcements (mm);
E_f elastic modulus of AFRP (MPa);
E_{sl} elastic modulus of longitudinal steel reinforcements (MPa);
E_{sh} elastic modulus of steel stirrups (MPa);
f_{c0} 28-day average compressive strength of unconfined plain specimens (MPa);
f_f tensile strength of AFRP (MPa);
f_l total equivalent confining stress (MPa);
f_{ls} equivalent confining stress due to the steel stirrups (MPa);

f_{lf} equivalent confining stress due to the AFRP jackets (MPa);
$f_{t\text{-}p}$ transitional strength for AFRP-confined reinforced HSC columns (MPa);
$f_{u\text{-}p}$ ultimate strength for AFRP-confined reinforced HSC columns (MPa);
f_{yl} yield strength of longitudinal steel reinforcements (MPa);
f_{yh} yield strength of steel stirrups (MPa);
k_e effectiveness coefficient for FRP confinement;
R corner radius of cross section (mm);
S_f width of AFRP jackets (mm);
S_f^* clear vertical spacing between adjacent AFRP jackets (mm, which is equal to zero for the columns confined with continuous AFRP wrapping);
S_h center to center spacing of steel stirrups (mm);
S_h^* clear vertical spacing between adjacent steel stirrups (mm);
t_f thickness of AFRP jackets (mm);
σ nominal axial stress (MPa);
ε nominal axial strain (m/m);
ε_{c0} compressive strain of unconfined plain specimens corresponding to f_{c0} (m/m);
ε_{fu} ultimate rupture strain of AFRP (m/m);
$\varepsilon_{t\text{-}p}$ transitional strain of AFRP-confined reinforced HSC columns (m/m);
$\varepsilon_{u\text{-}p}$ ultimate strain of AFRP-confined reinforced HSC columns (m/m);
ρ_{cc} ratio of area of longitudinal steel reinforcements to area of core of section.